

# Research on the Stability Problem of Hydroelectric Station Penstock under External Pressure Based on Neural Network

Chenghua Dang

Hebei University of Engineering  
Guangming South Street 199, Handan, Hebei, China  
CHINA  
dangchua@yahoo.com.cn  
Tieguo Ji

Hebei University of Engineering  
Guangming South Street 199, Handan, Hebei, China  
CHINA  
Rosemary1976@163.com  
Xinpei Jiang

Hebei University of Engineering  
Guangming South Street 199, Handan, Hebei, China  
CHINA  
Jangxinpei2007@163.com

*Abstract:* - The stability of steel penstock under external pressure is a main factor of penstock design in hydroelectric station. Since the assumption conditions and the boundary conditions are simplified in the currently existing methods, the obtained computing results have low accuracy level and every method has its limitation. In this present paper, we apply artificial neural network model and improved BP algorithm to this problem with more complicated conditions and factors. By analyzing the influences on losing stability and breach for reinforcing ring steel penstock caused by diameter-to-thickness ratio of the steel tube, size and space of reinforce rings, a new research approach is obtained and test results show this method is feasible and its validity is verified. This paper provides an efficient solving path for stability problem of reinforcing ring steel penstock under external pressure. Furthermore, we use this method to Chinese Yachihe hydroelectric power station design, the computing results show this method is reliable, economic and fully satisfies the project requirements.

*Key-Words:* - Penstock; Stability calculation under external pressure; Neural network; Simulated annealing algorithm

## 1 Introduction

Steel penstock is one of the key elements of hydropower station buildings. In recent years, steel penstock increasingly tends to large and gigantic scale due to a large number of high head and large capacity pumped storage power stations are constructed. With the application of a variety of high strength materials, steel penstock is gradually becoming thin-wall scale. For this thin-wall structure penstock, it is easy to lose its stability under external pressure and leads huge economic loss. Thus, its

anti-external pressure stability becomes more and more important, see [14-16] and the references therein.

It is well known that steel penstock is always accompanied by plastic deformation in the process of buckling instability, and always influenced by non-linear factors caused by dry shrinkage cracks of the outer wrapped concrete. These factors can make the highly nonlinear problem more complicated.

The stability analysis of stiffened penstock includes critical external pressure of reinforce ring calculation and shell between reinforce ring calculation. Currently when critical external pressure

of the penstock shell between reinforce ring is calculated, we always assume that the shell is consolidated in reinforce ring, namely, the stiffness of reinforce ring is infinite, without considering the influence of the size of stiffness of the reinforce ring impacted on critical external pressure of the shell; on the other side, when we compute critical external pressure of the reinforce ring, calculation accuracy is low because we do not consider the shell outside reinforce ring equivalent flange impacted on critical external pressure of reinforce ring (Such as S.Jacobsen France method) or did not consider accurately (Such as Amstutz method and Svoisky method). Recently Professor Liu in [5] presents a calculation method using semi-analytical finite element method to analyze the full instability of stiffened penstock shell, this method can objectively reflect the fact, but need a larger amount of calculation. In this paper, we first apply neural network model in [5, 6] and simulated annealing algorithm in [7] to simulate external pressure stability of reinforcing rings penstock. Comparing to the currently method such as grey theory and fuzzy theory and so on, artificial neural network owns its strong nonlinear power to handle all kinds of complex factors, see [10-14] and their references cited in these papers for the applications. It is well known that neural networks adjust their internal parameters by performing vector mappings from the input to the output space. Although they may achieve high accuracy of classification, the knowledge acquired by systems is represented in a large number of numerical parameters and network architectures, see [18] for the details. In order to overcome the drawback of neural network such as low convergence rate, easy to fall into local minimum and so on, in this paper, we combine an improved BP algorithm [18] and neural network to establish a new approach to the study of stability of penstock under external pressure and solve the problem with a variety of complex factors in the process of buckling failure of penstock.

## 2 Design Method of the Stiffened Penstock Shell Stability

### 2.1. Mises method

Mises hypothesizes the place of reinforcing ring being fixed. The losing stability deformation of penstock shell is along with circumference of the penstock and shows many waves. Its formula as follows (seen [9]):

$$P_{cr} = \frac{Et}{(n^2 - 1) \left( 1 + \frac{n^2 l^2}{\pi^2 r^2} \right)^2 r} + \frac{Et^3}{12(1 - \mu^2)r^3} \quad (1)$$

$$\times \left( n^2 - 1 + \frac{2n^2 - 1 - \mu}{1 + \frac{n^2 l^2}{\pi^2 r^2}} \right) \quad (2)$$

$$n = 2.74 \left( \frac{r}{l} \right)^{\frac{1}{2}} \left( \frac{r}{t} \right)^{\frac{1}{4}} \quad (2)$$

Bearing capacity of external pressure  $p$  is calculated by cylinder formula:

$$\sigma_s \cdot t = p \cdot r \quad (3)$$

Where  $p_{cr}$  -critical external pressure,  $n$  - breach wave numbers,  $t$  - thickness of penstock shell,  $l$  - distance of stiff rings,  $r$  - radius of penstock,  $E$  - elastic module  $\mu$  -Poisson ratio.

### 2.2. Numerical method

Due to error can not be avoided in manufacture and fixed process of penstock, thickness of penstock shell is asymmetry and there is initial crack between penstock and concrete. These factors lead to breach occurring in some defect place firstly. In this case, Mises method isn't worked. Although some breach examples of embedding penstock on engineering building and model experiment had proved the validity of hypothesis in Amstutz method [1] for losing stability wave shape  $\eta(\varphi) = a \cos(\varepsilon\varphi) + b \cos(\varphi) + c$ , Unfortunately, Amstutz method can be used only in mill finish steel tube. In 1990, professor Liu and Ma [5] proposed a semi-analytic finite element computing methods. This method plots the structure to cylinder shell element and cirque plate element. Element is connected by nodal circle among elements.

The stiffness equation of structure are as follows:

$$[K_E] + q[K_G^*]\{\Delta\} = \{P\} \quad (4)$$

$$[K_E] = \sum^e [K] \quad (5)$$

$$[K_E] = \sum^e (q^e / q) [K_G^*]^e \quad (6)$$

Where  $[K_E]$ ,  $[K_G^*]$  - elastic stiffness matrix and geometrical stiffness matrix  $e$  - The code of element;  $q$  - external pressure of structure;  $\{\Delta\}$ ,  $\{P\}$  - displacement vectors and nodal force vector of the structure.

If the determinant of total stiffness matrix

$([K_E] + q[K_G^*])$  is zero, the Characteristic equation of stability analysis are as follows :

$$| [K_E] + q[K_G^*] | = 0 \tag{7}$$

$$| [A] + \lambda[I] | = 0 \tag{8}$$

$$[A] = -[K_E]^{-1}[K_G^*] \tag{9}$$

$$\lambda = 1/q \tag{10}$$

The reciprocal of maximum characteristic root  $1/\lambda_{\max}$  is the losing stability loading.

For longer penstock shell and bigger distance of reinforcing ring, the calculating result of this numerical algorithm is consistent with Mises method. But for short shell, its result is 10%—15%. bigger than Mises method.

### 2.3. Lai-Fang Method

Lai-Fang method is proposed by Lai and Fang in [4]. They gave a derivation of expression by Amustz’s hypothetic condition. Its essential theory applies not only hypothesis of elastic theory but also more hypothesis as follows:

- ① The breach wave shape of penstock shell under external pressure shows 3 half of wave shape
- ② The reinforcing ring cannot move along to axis of penstock;
- ③ The longitudinal deformation is 0:  $U = 0$ ;

④The reinforcing ring is absolute stiffness. The author utilized boundary condition of losing stability of penstock to solved  $P_{cr}$  :

$$P = E' \frac{t}{r} \frac{\frac{1-\mu}{2} \lambda^2}{(\eta^2 - 1) \left( \frac{1-\mu}{2} \lambda^2 + \eta^2 \right)} + \frac{E'}{12} \left( \frac{t}{r} \right)^3 \left( \eta^2 - 1 + \frac{t}{3} \lambda^2 + \frac{\frac{16}{3} \lambda^4 + \frac{2}{3} \lambda^2}{\eta^2 - 1} \right) \tag{11}$$

Where  $\lambda = \frac{\pi r}{l}$  ;  $\eta = \frac{n\pi}{2\alpha}$ ,  $\alpha$  -The half deflection angle of breach wave shape for the center of cylinder shell.

By solving the equation  $dP/d\eta = 0$  , gain  $\eta$  value as follows Table 1, then calculate  $P_{cr}$  by expression (11).

In [4], professor Lai and Fang prove the reliability of the formula through experimentation. The results show: there is a good relationship between calculation value and experiment value when the distance of reinforcing ring is less ( $l = r$ ), but when  $l$  is biggish ( $l = 2r$ ), the computing result is 16.9% less than experiment value.

Table 1 The  $\eta$  value of the radial pressure approaching critical pressure.

$r/l$	$100t/r$											
	0.2	0.6	1.0	1.4	1.8	2.0	2.5	3.0	3.5	4.0	4.5	5.0
0.2	9.71	6.75	5.71	5.11	4.72	4.55	4.23	3.99	3.80	3.64	3.50	3.39
0.4	12.2	8.48	7.16	6.41	5.90	5.70	5.30	4.99	4.75	4.55	4.38	4.24
0.6	13.9	9.70	8.19	7.33	6.75	6.52	6.12	5.72	5.45	5.23	5.04	4.88
0.8	15.3	10.6	9.01	8.08	7.45	7.20	6.72	6.35	6.06	5.83	5.64	5.48
1.0	16.5	11.4	9.7	8.73	8.07	7.82	7.32	6.94	6.65	6.43	6.24	6.09
1.2	17.5	12.2	10.3	9.34	8.68	8.41	7.91	7.54	7.24	7.06	6.89	6.75
1.4	18.5	12.9	10.9	9.94	9.26	9.00	8.53	8.18	7.93	7.74	7.60	7.48
1.6	19.3	13.5	11.5	10.5	9.87	9.63	9.17	8.86	8.64	8.48	8.36	8.27
1.8	20.1	14.1	12.1	11.1	10.5	10.2	9.87	9.60	9.41	9.27	9.17	9.10
2.0	20.8	14.1	12.7	11.7	11.1	10.9	10.6	10.3	10.2	10.1	10.0	9.97
2.5	22.5	16.2	14.3	13.5	13.0	12.9	12.6	12.4	12.3	12.3	12.2	12.2
3.0	24.1	17.7	16.1	15.4	15.1	15.0	14.8	14.7	14.6	14.6	14.5	14.5

### 3. Simulation of the Stability Problem of Penstock under External Pressure

#### 3.1. Genetic - neural network method

We give more details of the specific genetic - neural network method used in the present paper as follows:

Step 1. Give an input and output sample.

Step 2. Set the network structure, initialize the network weights and thresholds. In this paper, we use this random function of Matlab to initialize the network weights and neuron threshold. Moreover, in order to avoid the saddle, we convert parameter value to interval  $[-1, 1]$ .

Step 3. Code scheme: Each of the network connection weights and neuron thresholds are directly presented by real numbers. Any a complete set of network weights and thresholds is equivalent to a chromosome of GA, and the initial population  $W$  consists of  $N$  chromosomes which are generated randomly. We define the population size of  $W$  as  $N$ .

Step 4. The objective function and fitness function: To travel the input sample forwards (propagation function is adapted as S-shaped hyperbolic tangent function) and to compute network actual output. Based on the actual output and the target output we calculate the global error as follows:.

$$E(W_i) = \sum_{j=1}^n \sum_{k=1}^{s^M} (t_k - y_k^{i,j})^2 \quad (12)$$

Where  $i = 1, 2, \dots, N$ ,  $y_k^{i,j}$  indicates the actual output of the  $k$ -th neuron in the output layer when the network parameter is  $i$ -th chromosome and the input of the network is sample  $j$ ;  $t_k$  is the target value of the  $k$ -th neuron of the output layer;  $n$  is the number of samples of the training set;  $s^M$  indicates the number of neurons of the output layer.

Fitness function is defined as a constant  $C$  multiplied by the reverse of the network objective function, its expression is shown as follows:

$$F(W_i) = \frac{C}{E(W_i)} \quad (13)$$

Where  $W_i$  is the  $i$ th chromosome of the populations.

Notation: It is well-known that the evolution goal of the genetic algorithm is fitness and the only way to evolution is along the direction which the fitness function is increasing, thus, the fitness function and the objective function should be converted. As the error of the evolution network is positive, we define the reverse of the objective function as fitness function. Moreover, in order to ensure the fitness function value is not too

small, we induce a constant  $C$  to the expression.

Step 5. To determine the population size  $N$ , cross probability  $p_c$ , variation probability  $p_m$ , the number of network Layer  $M$  and the neuron number in each layer.

Step 6. To choose the initial population which is generated randomly:  $W = \{W_1, \dots, W_i, \dots, W_N\}$

Step 7. Fitness calculation: For any a given couple of input and output samples, the globe error of network is computed by equation (12), and we use equation (13) to calculate the fitness of each chromosome.

Step 8. Population selection operation: We select a individual by roulette wheel method and compute the fitness of the individual; To convert the individual's fitness value to selected probability in proportion as

$$P_s(W_i) = \frac{F(W_i)}{\sum_{i=1}^N F(W_i)}$$

probability  $sumPs_i$  depending on the chosen probability

as  $sumPs_i = \sum_i P_s(W_i) \quad i = 1, 2, \dots, N$ ;  $N$  length random

vector is generated from the interval  $(0, 1)$ , if a random number  $r$  of the vector meets  $sumPs_{i-1} < r \leq sumPs_i$ , the  $i$ th chromosome is selected as an element;  $N$  chromosomes are selected to form the mating pool for reproduction based on the rule above. If the chromosome with the largest fitness value of the populations is not selected, then the chromosome is directly used to replace the chromosome with the smallest fitness value in the pool..

Step 9. Cross operation: According to the cross probability of  $p_c$ , the number of individuals which are generated by cross operation  $p_c \times N$  is calculated. We repeat the following process to obtain the parent of cross operation: a length  $N$  random numbers  $R = (r_1, r_2, \dots, r_n)$  is generated from the interval  $(0, 1)$ ; if  $r_i < p_c$ ,  $W_i$  is selected as a parent, we can choose  $p_c \times N$  chromosomes as the parents. We denote such selected chromosomes by  $W'_1, W'_2, \dots$ , pair and crossed them randomly like this:  $(W'_1, W'_2), \dots, (W'_{p_c \times N - 1}, W'_{p_c \times N})$ .

We take  $(W'_1, W'_2)$  for example and show the process of cross operation.

Assumed that  $W'_1 = A_{11}A_{12} \dots A_{1l}$ ,  $W'_2 = A_{21}A_{22} \dots A_{2l}$  ( $l$  is the length of chromosome), we define a random number sequence  $c = c_1c_2 \dots c_l$  as a sample, which is generated from the interval  $(0, 1)$  and its length is  $l$ . The new individuals are obtained as

$W'_{1n} = A'_{11}A'_{12} \cdots A'_{1l}$ ;  $W'_{2n} = A'_{21}A'_{22} \cdots A'_{2l}$  after crossing by the following formulas:

$$A'_{1i} = \begin{cases} \alpha A_{1i} + (1-\alpha)A_{2i}, & c_i < 1/2 \\ \beta A_{1i} + (1-\beta)A_{2i}, & c_i \geq 1/2 \end{cases}$$

$$A'_{2i} = \begin{cases} \alpha A_{2i} + (1-\alpha)A_{1i}, & c_i < 1/2 \\ \beta A_{2i} + (1-\beta)A_{1i}, & c_i \geq 1/2 \end{cases}$$

Where :  $\alpha$ 、 $\beta$  are random numbers.

After cross is finished, we compare the new individual's fitness value with the parent fitness value. In order to obtain a good individual, a pair of parent individuals is used to conducted a number of cross, until at least one cross-individual fitness value is better than the parent after, Replace  $W'_1, W'_2$  of the parent with  $W'_{1n}, W'_{2n}$ .

Step 10. Variation operation: Based on variation probability, the number of variable chromosome of the population  $p_m \times N$  is calculated. How to select variable individual is as follows:

To compute fitness value of new population which is formed after selection and cross operation; and then calculate the selection probability of each chromosome defined as  $select\_P_s$ , the selection probability of each chromosome is defined as  $select\_P_m = (1 - select\_P_s) / (N - 1)$ , ( It implies that namely the chromosome with smaller fitness value is selected to vary; at the end, we construct a parent of variation which consist of  $p_m \times N$  chromosomes chosen by roulette wheel method.

Offspring is produced after variation is

$$A'_m = A_m + \gamma \times D \times d$$

Where  $\gamma$  is a random number of the interval ( 0 , 1 ) ,  $d$  is a sequence of random numbers which has the same dimension as the length of the chromosome.  $D$  is a direction factor. In order to pursue a good variation, we make many times variation until the variable individual's fitness value is greater than the parent fitness value. Thus, a new population is generated.

Step 11. Return to step 4 until the network is convergence

Step 12. Use the convergence network to inspect the test sample, if the accuracy does not meet the requirement, return to step 2 to repeat till the accuracy requirements are obtained.

### 3.2. The computing sample data

The computing model of the stability analysis of the penstock shell under external pressure is shown in Fig.1. The rolled steel adopts 16Mn , (elastic module

$E = 2.1 \times 10^5 \text{ Mpa}$  , Poisson ratio:  $\mu = 0.3$  ,  $\sigma_s = 340 \text{ Mpa}$  ), The ratio of the penstock radius  $r$  to penstock thickness shell  $t$  ( relatively radius  $r/t$  ) is from 20 to 400, step length: 20, The ratio of distance of reinforcing ring  $l$  to penstock radius  $r$  ( relatively distance of reinforcing ring  $l/r$  ) : [ 0.1, 0.2, 0.3, 0.5, 0.8, 1.4, 2.0, 3.0, 40 ] , total have 180 models.

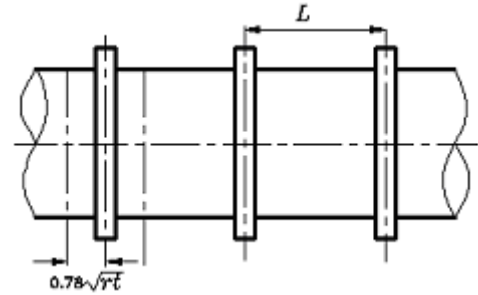


Fig.1. The figure of reinforcing ring penstock.

By formula (1), (2) to calculate critical external pressure  $p_{cr}$  and wave numbers  $n$  of losing stability

### 3.3. Simulation

In the paper, we select four layers BP neural networks, input layer has 3 neuron ( relatively radius  $r/t$  , relatively distance of reinforcing ring  $l/r$  , wave number of losing stability  $n$  ) , the neuron number of two hidden-layer are respectively 11 and 4, the output layer is critical pressure ( seen [2] ). The structure of network is shown in Fig.2. The neuron transfer function is the Sigmoid differentiable function, the outputs neuron use the Purlin linearity transfer function. The neural network sample data is obtained by formula (1), ( 2 ) . We use improved BP algorithm and simulated annealing method to train the network ( Vogl, [8]; Dong *et al.*, [2]; Dong *et al.*, [3]).

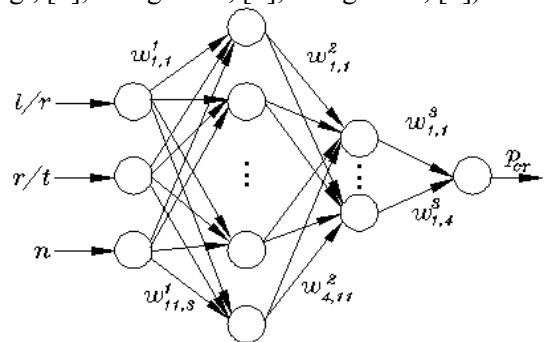


Fig.2. The structure of neural network.

The training process of the neural network is shown in Fig.3.

The above-mentioned models are tested by using convergent network , the computing results is shown by Table 2.

The computational result fitting figure of simulation and Mises theory is as follows Fig 4.

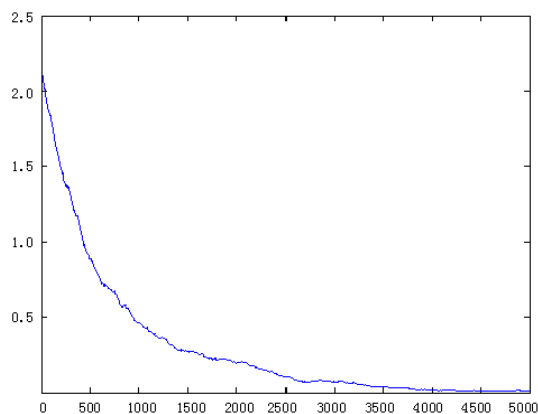


Fig.3. The evolvement process of BP network.

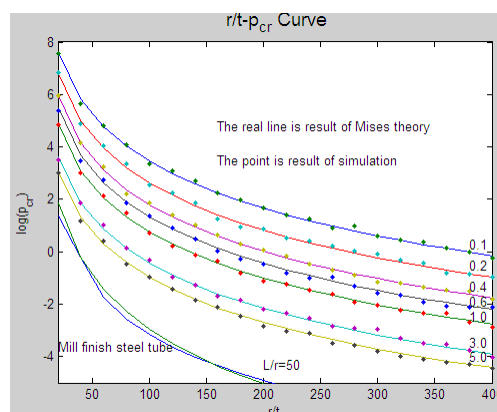


Fig. 4. Fitting figure of the computational result of simulation and Mises theory.

Table 2 The part calculating result of critical pressure.

Critical pressure $P_{cr}$ (Mpa)		$l/r$				
		0.1	0.2	0.3	0.5	0.8
(simulation)						
$r/t$	20	2024.26 (2024.21)	901.87 (901.90)	554.56 (554.52)	299.14 (299.14)	170.36 (170.40)
	60	119.16 (119.17)	52.05 (52.14)	31.97 (31.89)	17.43 (17.56)	10.12 (10.18)
	100	31.71 (31.57)	13.79 (13.71)	8.50 (8.43)	4.67 (4.71)	2.74 (2.77)
	140	13.23 (13.38)	5.75 (5.86)	3.55 (3.47)	1.97 (2.01)	1.16 (1.14)
	180	6.88 (6.92)	2.99 (2.87)	1.86 (1.79)	1.03 (1.03)	0.61 (0.67)
	260	2.64 (2.57)	1.16 (1.23)	0.72 (0.78)	0.40 (0.37)	0.24 (0.28)
	300	1.82 (1.81)	0.79 (0.81)	0.49 (0.51)	0.28 (0.25)	0.16 (0.16)
	360	1.13 (1.14)	0.49 (0.45)	0.31 (0.29)	0.17 (0.19)	0.11 (0.15)
	400	0.86 (0.81)	0.37 (0.36)	0.24 (0.23)	0.13 (0.11)	0.08 (0.07)

#### 4. Calculated Result Analysis

1) Fig.4 shows: with an increasing of  $r/t$  ,the losing stability capability of penstock under external pressure is decrease acutely. The critical external pressure  $P_{cr}$  decrease with an increasing of  $r/t$  .

Within  $r/t=20 \sim 260$ ,the critical external pressure is

acutely decrease, beyond the range, the change is less. For example: within  $l/r=0.1 \sim 3.0$ ,  $r/t$  from 20 to 260,  $P_{cr}$  will decrease 0.13% ~ 0.16% of initial value ( $r/t=20$ ,  $P_{cr}$ ); When the diameter of penstock is increased to a certain value, the stability power of the penstock under external pressure will change very less. For example:  $L/r=3.0$ ,  $r/t=400$ , the  $P_{cr}$  value is only 0.02 Mpa.

2) The calculated result shows: The critical pressure  $P_{cr}$  of penstock decrease with relatively distance of reinforcing ring  $l/r$  increasing, but the influence of decreasing velocity is less than relatively radius  $r/t$ . For example:  $r/t=300$ ,  $l/r=0.1 \sim 3.0$ , the critical external pressure  $P_{cr}$  will decrease 2.19% ~ 43.41% of initial value.

3) The most effective reinforcing ring's space: The curve of Fig.4 shows: reducing the distance of reinforcing ring can effectively increase the critical external pressure  $P_{cr}$  value, and while  $L/r$  decrease,  $P_{cr}$  value and its increase ratio increase. For example:  $r/t=260$ ,  $l/r$  from 3.0 decrease 0.8 and continue to decrease 0.1, the increment of  $P_{cr}$  is respective 0.18 Mpa and 2.40 Mpa. In another word, the distance of reinforcing ring reduce  $0.1r$ , the average increment of  $P_{cr}$  value is respective 0.0082 Mpa, 0.34 Mpa. The latter is 41 multiples of the former. So the most effective distance of reinforcing ring is  $L < 0.8r$ . The reinforcing ring distance of SanXia hydropower station is:  $L=0.32r$ .

4) Non effective distance of reinforcing ring: The Fig.4 shows: with an increasing of the distance of reinforcing ring, the function of reinforcing ring decrease. While  $L/r=40$ , the  $\log(p_{cr}) \sim r/t$  curve of reinforcing ring penstock and mill finish steel tube (the calculate formula of the mill finish steel tube:  $p=2E(t/D)^3$ ,  $D$ : diameter of steel tube) is almost superposition. This shows that the losing stability power under external pressure of these tubes are same, then the reinforcing ring does not possess any sustaining effect on the stiffness.

5) The losing stability wave number: The losing stability wave number  $n$  is a synthesis embodiment for longitudinal and circular stiffness of the penstock. With an increasing of the penstock diameter, the stiffness of circular decrease, the losing stability wave number increase. But in axial direction, with an

increasing of the reinforcing ring's space, the axial stiffness decrease and  $n$  is less. For the penstock of big diameter and thick space, the losing stability wave shape shows the form of more waves, but for the sparse space and small diameter is the form of less wave.

6) The design of penstock: Fig.4 shows: the curve cluster of ' $\log(p_{cr}) \sim n$ ,  $r/t \downarrow l/r$ ' are divided two district of upper and lower by the plastic losing stability curve. If the penstock diameter and relatively reinforcing ring's space are biggish, the penstock appears elastic losing stability under smaller external pressure;  $\log(p_{cr})$  value locates the district below the elastic losing stability curve. But the penstock diameter and relatively distance of reinforcing ring are less, the stability power of penstock under external pressure is powerful and can bear great pressure; the  $\log(p_{cr})$  value locates the district upon the elastic losing stability curve. When we design the penstock, if  $r/t$  value has been confirmed by the demand of using and building, we may select appropriate  $l/r$  value according to Fig.4, so that the critical external pressure meet anti-external pressure request and be close to the losing stability curve.

## 5. Numerical example

The design conditions of the stabilization of underground penstock under external pressure of Yachihe Hydropower Station Diversion Project China consist of venting and maintenance condition and construction condition. The normal external water pressure head of venting and maintenance condition:  $H_1=50\text{m}$ , the normal external water pressure head of checking condition:  $H_2=80\text{m}$ , the Grouting pressure of construction condition:  $P=0.3\text{Mpa}$ .

Under the above design conditions, the maximum external water pressure head is 80m (namely: 0.80Mpa), the design external pressure of the underground penstock external pressure stability is  $K \times 0.80\text{Mpa}$ , where  $K$  is safety factor. For stiffened steel penstock, reinforce ring and the shell between rings, the safety factor  $K$  is 1.8, thus in this numerical example, the design external pressure of the penstock is  $1.8 \times 0.80=1.44\text{Mpa}$ .

1) The stability design of penstock shell

The stability design of the stabilization of the underground penstock under external pressure of Yashuihe Hydropower Station Diversion Project is divided into the stability design of circumference shell and reinforce ring. Mises, Lai-Fang Method in [4], Semi-analytical finite element method for cylindrical shell and artificial neural network simulated model are used to solve the stability design of circumference shell ; the stability design of reinforce ring is calculated by formula (12) as follows:

$$p_{cr} = 3EJ_k / R_k^3 L \quad (12)$$

Where,  $p_{cr}$  is the value of external pressure,  $R_k$  is radius of gravity axis center of effective section of the reinforce ring,  $J_k$  is inertia moment of of gravity axis center of effective section (  $\text{mm}^4$  )

When using semi-analytical finite element method to make stability design, freely-supported effect and mounted effect of reinforce rings should be separately considered.

In the stability design of penstock shell, the radius of steel tube:  $r = 2.5m$  , the space of reinforce rings:  $l = 2.0m$  , The rolled steel: 16MnR , elastic modulus:  $E = 210Gpa$  , Poisson's ratios:  $\mu = 0.3$  , Yield

Strength:  $\sigma = 325Mpa$  , the initial gap between steel tube and concrete:  $\Delta = 0.5mm$  .

Several calculation methods above are used to calculate the stabilization of underground stiffened penstock under external pressure of Yachihe Hydropower Station, the results are shown in Table3.

The results can be seen from the above that the calculation solved by Mises method is between the calculations concerned freely-supported effect and mounted effect solved by semi-analytical finite element method. So Mises method can be used as a main method to calculate the stabilization of underground stiffened penstock under external pressure, while the calculation of Lai-Fang Method is high.

The results show that when thickness of penstock shell between the rings is 20mm and 22mm, the calculation safety factor solved by reinforce ring simply supported semi-analytical finite element method is less than 1.8 that can not meet the requirements. But this method takes into account the capacity of resisting external pressure of steel penstock in the case of reinforce ring failure, and the actual capacity of resisting external pressure of steel penstock should be greater than this value. The

Table 3 The calculation results of the stabilization of underground stiffened penstock of Yachihe Hydropower Station.

Thickness of shell	Mises		reinforce ring simply supported semi-analytical finite element method		reinforce ring mounted semi-analytical finite element method		Lai-Fang Method		neural network	
	Buckling pressure Mpa	Safety factor	Buckling pressure Mpa	Safety factor	Buckling pressure Mpa	Safety factor	Buckling pressure Mpa	Safety factor	Buckling pressure Mpa	Safety factor
20	1.529	1.91	0.859	1.07	1.595	1.99	2.716	3.40	1.517	1.89
22	1.965	2.46	1.144	1.43	2.123	2.65	3.462	4.33	1.903	2.38
25	2.690	3.36	1.678	2.10	3.115	3.89	4.795	5.99	2.716	3.39
27	3.266	4.08	2.114	2.64	3.924	4.91	5.846	7.31	3.461	4.32
29	3.926	4.91	2.619	3.27	4.862	6.08	7.031	8.79	4.192	5.24

Note: 1 .Units of thickness of shell, Thickness Of Ring plate and Height of Ring plate are mm.

2.The results calculated by neural network model are basically consistent with the ones calculated by Mises method.

Table 4 The calculation results of the stabilization of underground stiffened penstock and reinforce ring of Yachihe Hydropower Station China.

Thickness of shell	Thickness Of Ring plate	Height of Ring plate	Instability of reinforce ring	
			buckling pressure Mpa	Safety factor
20	20	300	2.380	2.98

22	22	300	2.685	3.36
25	25	300	3.159	3.95
27	27	300	3.468	4.36
29	27	300	3.823	4.78

Note: Units of thickness of shell, thickness of ring plate and height of ring plate are mm.

calculation safety factor solved by other methods is greater than 1.8 that meets the requirements. For security purposes, reinforce ring can be adjusted to the spacing of 1.5m on the tube sections where the thickness of penstock shell is 20mm and 22mm. Meanwhile, the calculations solved by reinforce ring simply supported semi-analytical finite element method are 1.557Mpa (safety factor is 1.95) and 2.072Mpa (safety factor is 2.59) that meet the requirements.

## 2) Unsteady buckling analysis of reinforce ring

Set the size of reinforce ring, calculate compression-bending critical external pressure of it by equation (12), and the results are shown in Table 4.

Seen from Table 4, when the radius of penstock shell is 2.5m, the spacing of reinforce ring is 2.0m, the thickness of penstock shell is 0.02m, we obtain the height of reinforce ring is 0.3m,

$P_{cr} = 2.380\text{Mpa}$ . The reinforce ring is steady follows from  $P_{cr} = 2.380\text{Mpa} > 1.44\text{Mpa} (K \times 0.8)$ .

When the thickness of penstock shell is 0.022m, the compression-bending critical external pressure  $P_{cr} = 2.685\text{Mpa}$ , The stability of reinforce ring is more reliable.

The following conclusions of the stabilization of underground penstock under external pressure of Yachihe Hydropower Station Diversion Project were drawn: on venting and maintenance condition and construction condition special load combination (

$H_2 = 80\text{m}$ ) condition, the thickness of penstock shell is 20mm, the radius of penstock shell is 2.5m, the rolled steel is 16MnR ( $E = 210\text{Gpa}$ ,  $\mu = 0.3$ ,  $\sigma = 325\text{Mpa}$ ); reinforce ring (The form of reinforce ring is a rectangular, the spacing of ring:  $l = 0.8 \times r = 2\text{m}$ , the size of reinforce ring: thickness: 20mm, height: 300mm) is not only economic and reasonable, but also meets the project requirements.

## 6. Conclusion

The paper analyzed characteristic and drawbacks of different calculating method of stability problem of penstock shell under external pressure. We apply artificial neural network model and improved BP algorithm to this problem with more complicated conditions and factors. By analyzing the influences on losing stability and breach for reinforcing ring steel penstock caused by diameter-to-thickness ratio of the steel tube, size and space of reinforce ring, a new approach and a simulation method are proposed. The feasibility is proved by tested sample and the application on design of Chinese Yahechi hydroelectric station project. The algorithm provides a new approach for the design of embedding reinforcing penstock in the hydropower station building engineering. It possesses reference value in solving high dimension non-linear optimization problem on water conservancy and electric power engineering.

## Acknowledge

Authors thank professor Wensheng Dong for his helpful suggestion and this paper is supported by Chinese NSF (10971046).

## References:

- [1] Amstutz E., Buckling of pressure-shaft and tunnel linings, *International Water Power and Dam Construction*, Vol.22, No.11, 1970, pp.391-399.
- [2] Dong, W.S., Dang, C.H., Deng, Z.C., Liu, D.C., Stability Analysis of Penstock under External Pressure Based on GA-NN, *Chinese Journal of Applied Mechanics*, Vol.23, No.2, 2006, pp.304-307.
- [3] Dong, W.S., Deng, Z.C., Liu, D.C., Liang, Y.P., A relatively simple and fast method for calculating critical uniform external pressure of steel cylindrical shell structure, *Journal of Northwestern Polytechnical University*, Vol.24, No. 1, 2006, pp.119-123.
- [4] Lai, H.J., Fang, C.R., The investigate of losing stability ang breach for emmbeding reinforcing

- rings penstock under external pressure, *Journal of Hydraulic Engineering*, Vol.12, 1990, pp.30-36.
- [5] Liu, D.C., Ma, W.Y., Research on the semi-analytical finite element methods analyzing stability of cylindrical shells external pressure, *Proceedings of International Conference on Structural Engineering and Computer*, 1990, pp.1397-1402.
- [6] Martin, T.H., Menhaj., M., Training feedforward networks with the Marquardt algorithm, *IEEE Transactions on Neural Networks*, Vol.5, No.6,1994, pp.989-993.
- [7] Metropolis, N., Rosenbluth, A.W., Rosenbluth, M.N., Teller, A.H., Teller, E., Equation of state calculations by fast computing machines, *Journal of Chemical Physics*, Vol.21, No.6, 1953,pp.1087-1092.
- [8] Vogl, T.P., Mangis, J.K., Zigler, A.K., Zink, W.T., Alkon., D.L., Accelerating the convergence of backpropagation method, *Biological Cybernetics*, Vol.59, No.2,1988,pp.256-264.
- [9] Wang, P.F., Chen, M.J., Chen, J.T., *Design specification for steel penstock of hydroelectric station (SL281-2003)*, The ministry of water resources of The People's Republic of China, 2003. pp. 251.
- [10] L. Merad, M. Bensaada, Radial basic function neural networks estimation of battery performance, *Computers and Simulation in Modern Science*, Vol. II, WSEAS Press, pp.114-117.
- [11] Y. F. Hsiao, Y. S. Tarn and K. Y. Kung, Comparison of the grey theory with neural network in the rigidity prediction of linear motion guide, *WSEAS Transactions on Applied and Theoretical Mechanics*, Issue 1, Vol. 4 Jan. 2009, pp.25-41.
- [12] Y. F. Hsiao, Y. S. Tarn, Study of the lubrication oil consumption prediction of linear motion guide through the grey theory and the neural network, *WSEAS Transactions on Applied and Theoretical Mechanics*, Issue 1, Vol. 4 Jan. 2009, pp.42-51.
- [13] H. Kahramanli and N. Allahverdi, A system for detection of liver disorders based on adaptive neural network and artificial immune system, *Proceedings of the 8th WSEAS international conference on applied computer science*, 2008, pp.25-30.
- [14] Amstutz E., Buckling of pressure-shaft and tunnel linings. *International Water Power and Dam Construction*, 1970, 22(11), pp.391-399.
- [15] Jacobsen S. Buckling of pressure tunnel steel linings with shear connectors. *International Water Power and Dam Construction*,1968,20(6), pp.58-62.
- [16] Jacobsen S. Pressure distribution in steel lined rock tunnels and shafts. *International Water Power and Dam Construction*, 1977,29(12), pp.47-51
- [17] Sun, F Shi, Design of BP Networks Based on MATLAB, *Computer and digital Engineering*, 2007, 35(8), pp.124-126.
- [18] J. A. Freeman, D. M. Skapura, *Neural networks: Algorithms, Application and programming Techniques*, Addison-Wesley, New York, 1991.